

GRAIN BOUNDARY SLIDING IN IRON: EFFECT OF VACANCY

Eva Vitkovská¹, Peter Ballo¹

*¹Institute of Nuclear and Physical Engineering, Faculty of Electrical Engineering and Information Technology, Slovak University of Technology in Bratislava, Ilkovičova 3, 812 19 Bratislava 1, Slovak Republic
E-mail: eva_vitkovska@stuba.sk*

Received 25 April 2016; accepted 10 May 2016

1. Introduction

Grain boundary (GB) sliding is considered to be one of the principal mechanisms of plastic deformation for polycrystalline materials. Therefore, an improved understanding of GB-based plastic deformation is crucial for the design of new nanostructured as well as conventional polycrystalline metals. The effect of GB sliding can be described as the relative displacement of two adjacent grains in the direction parallel to the boundary interface. The sliding is often accompanied by migration of the boundary parallel to itself [1] and connected with propagation of GB dislocations [2]. Connection between in-plane translation (b) and normal boundary displacement (m) is characterized by coupling factor $\beta=b/m$ [1]. Segregation of impurities and defects on GBs changes the structure of GB at the atomic level and consequently effects GB sliding behaviour. Close attention is given to a vacancy effect on sliding of bcc-iron (α -iron) GBs [2-4]. Zhou et al. [3] showed using first principles calculation, that presence of vacancy on GB weakens the interfacial bonding and decreases sliding energy barrier. Result is consistent with result obtained for copper GBs [5]. Another group [4] using first principles calculation identified vacancies as heterogeneous nucleation sites which activate GB dislocation loops and consequently promote GB migration. Hyde et al. [2] applied molecular dynamic simulation and showed reduction in the sliding resistance due to vacancy segregation.

The aim of our work is to investigate the influence of GB vacancy segregation on GB energy, sliding energy profile and coupling factor. The investigation was made on four $\langle 100 \rangle$ -symmetric tilt GBs in bcc-iron: $\Sigma 5(210)$, $\Sigma 5(310)$, $\Sigma 17(410)$ and $\Sigma 13(510)$. The article is arranged as follows: computational details are summarized in Sec. 2, results are presented and discussed in Sec. 3 and main contribution of our work is summarized in Sec. 4.

2. Methodology

Grain boundary supercells were constructed according to coincidence site lattice (CSL) theory. Two ideal bcc-crystals were rotated towards each other around the [001] rotation axis and matched together. This geometry in combination with periodical boundary conditions creates computational cell which contains two GBs. First of them is positioned in the middle of the computational cell while second is from geometrical reasons split into two parts positioned on the top and bottom edge of the cell. GB structure was optimized by our newly developed optimization algorithm OPSA (Optimization by Parallel Simulated Annealing) which is in fact combination of parallel simulated annealing (SA) and genetic algorithm. Note, in our configuration, both GBs were optimized. Supercell parameters are summarized in Tab.1.

Sliding process was realized quasi-statically. Atoms in supercell were divided into two groups: stable and mobile. Each group had equal number of atoms. Mobile grain was rigidly shifted along GB plane. SA optimization was applied after each rigid shift. Annealing

ran from 850 K temperature to 10 K using a stepwise exponential decrease of temperature involving a total of 350 steps. At the end temperature of 0 K was reached by an acceptance of the position of atoms with lower energy. Shifting process was carried out in two different ranges: In the range of 0 to 50% CSL lattice period divided into 25 steps and in the range of 0 to 2 Å divided into 11 steps. To stabilize shifting process we excluded from SA optimization few atoms placed between middle and edge GB. Number of atoms excluded from optimization and number of atoms belonging to mobile group is listed in Tab. 1.

Tab. 1. Parameters of α -iron grain boundary supercells. Number of atoms (N), number of mobile atoms (N_m), number of atoms excluded from optimization (N_f) and supercell dimensions (sx , sy , sz). Dimension (sy) corresponds to CSL period

	N	N_m	N_f	$sx[\text{Å}]$	$sy[\text{Å}]$	$sz[\text{Å}]$
$\Sigma 5(210)$	64	32	10	2.855	6.384	40.857
$\Sigma 5(310)$	84	42	16	2.855	9.028	37.919
$\Sigma 17(410)$	112	56	18	2.855	11.772	38.777
$\Sigma 13(510)$	140	70	24	2.855	14.558	39.194

In order to investigate effect of vacancy on GB mobility we prepared special supercells containing one vacancy. The vacancy was placed in the plane adjacent to GB plane, which was positioned in the middle of the supercell. This plane was in our previous calculations identified as plane most favorable for vacancy formation. The sliding process was realized in the same manner as was described for GB supercells without vacancy. GBs without vacancy we will refer as clear.

Atomic interaction at microscopic level was described by Embedded-atom method (EAM) [6] potential and we used parametrization provided by Mendeleev et al. [7] According this parametrization was lattice parameter set to 2.855 Å. The advantage of EAM is that it allows to compute energy of each individual atom. Consequently, it is possible to compute energy of middle and edge GB separately. We divided supercell into two parts: one containing atoms which z -coordinate meets condition $|z| < sz/4$ and another one containing atoms which z -coordinate meets condition $|z| > sz/4$. Note, z is direction perpendicular to GB plane, initial GB plane was placed at $z = 0$ and sz is supercell dimension in z -direction. Each part contains N atoms. In this instance GB energy is given by equation:

$$E_{GB} = \frac{E_{GB}^N - NE_c}{sxsy} \quad (1)$$

where E_{GB}^N is total energy of atoms assigned to middle GB, E_c is cohesive energy and $sxsy$ is GB area. After removal of one atom from middle GB plane the vacancy formation energy is defined as:

$$E_{vf} = E_{GB}^N - E_{GB}^{N-1} + E_c \quad (2)$$

where E_{GB}^{N-1} is total energy of atoms assigned to middle GB after removal of one atom. The GB sliding energy barrier is defined as:

$$\Delta E = E_{gb}^0 - E_{gb}^b \quad (3)$$

where E_{gb}^b and E_{gb}^0 are GB energies with and without GB shift.

3. Results and discussion

Comparison of GB sliding energy profiles obtained for GBs with and without vacancy is in Fig. 1-2. First of them displays grain displacement from 0 to 50% of CSL period and second one displays grain displacement from 0 to 2Å. A common feature of all profiles is an occurrence of several local maxima followed by local minima. Transition from local maxima to local minima is coupled with GB migration. Maximal value of energy profile is called sliding barrier. Displacement between two neighboring minima (or maxima) is called migration period. Migration distance is defined as normal boundary displacement connected with migration period. Energy barrier, migration period and migration distance of GBs was identified from energy profiles in Fig. 2. Coupling factor, ratio of migration period to migration distance, was derived from both, profiles in Fig. 1 and profiles in Fig. 2. In the case of profiles in Fig. 1, where are several local maxima, coupling factor was computed as total displacement divided by total migration distance. The total displacement consists of several migration periods. Total displacement was limited to 30% of CSL period. The reason of limitation is, that at 30% displacement the GB plane migrates very close to atoms excluded from optimization process. These atoms act as barrier for migration process which results in sharp increase of GB energy observed in case of GB $\Sigma 17(410)$ and $\Sigma 13(510)$.

GB energies, sliding barriers, migration periods, migration distances and coupling factors of clear GBs are listed in Tab. 2. GB energies of clear GBs are in good agreement with result obtained by Terentyev et al. [8] and Tschopp et al. [9]. GB energies, vacancy formation energies, sliding barriers and coupling factors of GBs with vacancy are listed in Tab. 3. There are also trends of the effect of vacancies on GB energy, sliding barrier and coupling factor in Tab. 3.

Tab. 2. Grain boundary energy (E_{GB}), sliding barrier (ΔE_m), migration period (b), migration distance (m) and coupling factor (β) of α -iron $\langle 100 \rangle$ symmetric tilt grain boundaries

	$E_{GB}[\text{Jm}^{-2}]$	$\Delta E_m[\text{Jm}^{-2}]$	$b[\% a_{\text{csl}}]$	$b[\text{\AA}]$	$m[\text{\AA}]$	$\beta^{(11)}$	$\beta^{(25)}$
$\Sigma 5(210)$	1,468	0,117*	25,6	1,636	1,257	1,302	0,601
$\Sigma 5(310)$	1,050	0,336	18,1	1,636	2,674	0,612	0,679
$\Sigma 17(410)$	1,120	0,374	12,4	1,455	2,754	0,528	0,658
$\Sigma 13(510)$	1,083	0,207	7,49	1,091	2,700	0,404	0,425

⁽¹¹⁾ shift from 0 to 2 Å in 11 steps ⁽¹²⁾ shift from 0 to 50% of CSL period in 25 steps

Tab. 3. Grain boundary energy (E_{GB}), vacancy formation energy (E_{vf}), sliding barrier (ΔE_m) and coupling factor (β) of α -iron $\langle 100 \rangle$ symmetric tilt grain boundaries with vacancy. Effect of vacancy on grain boundary energy, sliding barrier and coupling factor: (↓) decrease, (↑) increase, (–) no impact

	Parameters					Trends		
	$E_{GB}[\text{Jm}^{-2}]$	$E_{vf}[\text{eV}]$	$\Delta E_m[\text{Jm}^{-2}]$	$\beta^{(11)}$	$\beta^{(25)}$	E_{GB}	ΔE	β
$\Sigma 5(210)$	1,128	-0,375	0,306 ⁽¹¹⁾	-	0,940	↓	↑	↑
$\Sigma 5(310)$	1,329	0,451	0,416	0,743	0,707	↑	–	↑
$\Sigma 17(410)$	1,110	-0,027	0,312	0,712	0,664	–	↓	↑
$\Sigma 13(510)$	1,0811	0,014	0,207	0,474	0,528	–	↓/–	↑

⁽¹¹⁾ shift from 0 to 2 Å in 11 steps ⁽¹²⁾ shift from 0 to 50% of CSL period in 25 steps

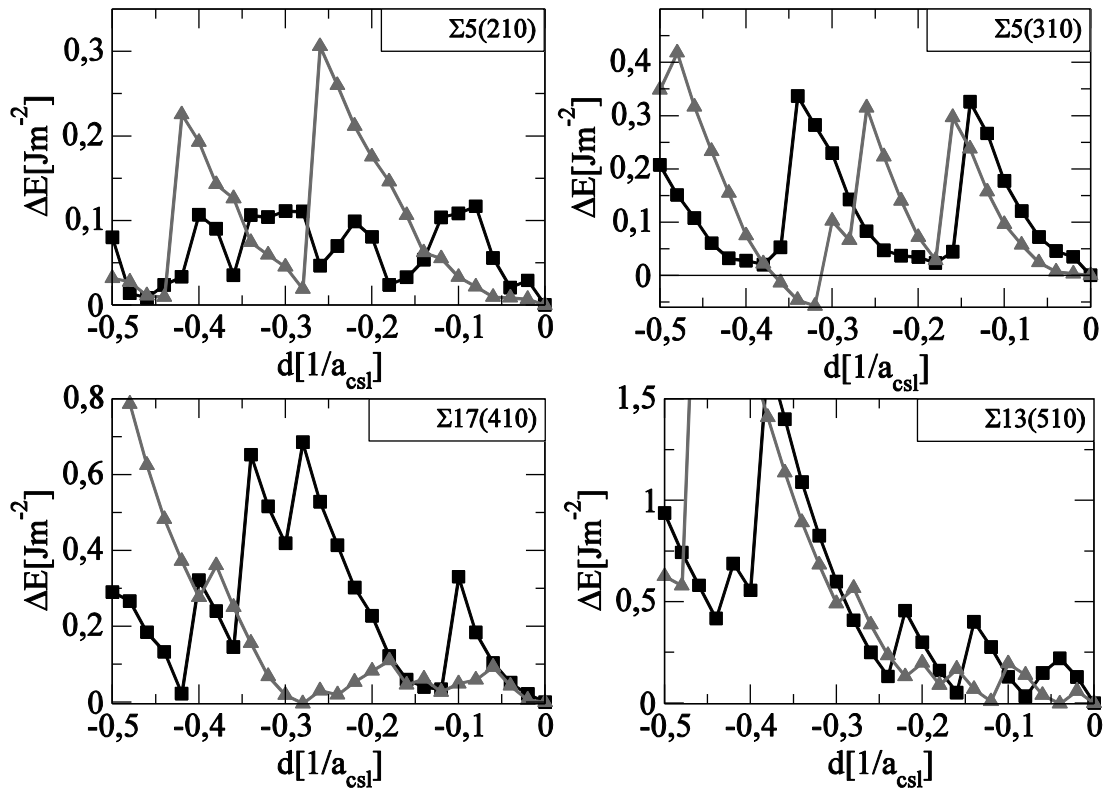


Fig. 1: Sliding energy profiles of α -iron $\langle 100 \rangle$ symmetric tilt grain boundaries without (squares) and with (triangles) vacancy. Sliding distance was set from 0 to 50% of CSL lattice period (a_{CSL})

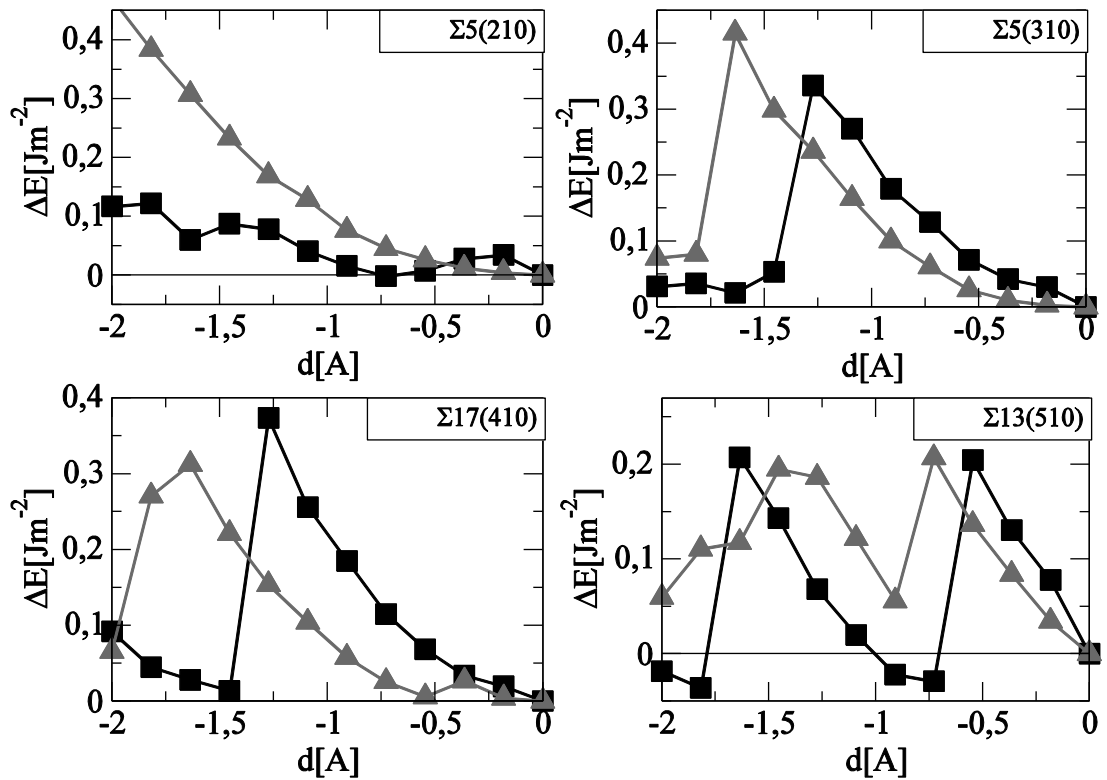


Fig. 2: Sliding energy profiles of α -iron $\langle 100 \rangle$ symmetric tilt grain boundaries without (squares) and with (triangles) vacancy. Sliding distance was set from 0 to 2\AA

A clear trend, increase, was identified only in the case of coupling factor. Formation energies of vacancies positioned at low coincidence site GBs $\Sigma 17(410)$ and $\Sigma 13(510)$ are close to zero what implies no impact on GB energy. Based on energy profiles in Fig 1., we can conclude, that vacancy segregation on these GBs lowers sliding barrier. However, this trend is not so significant from profiles in Fig. 2. No impact of vacancy on sliding barrier was observed for GB $\Sigma 5(310)$. This GB is also GB with highest vacancy formation energy. Contradictory, GB $\Sigma 5(210)$ has lowest (negative) vacancy formation energy. Creation of vacancy at GB $\Sigma 5(210)$ leads to significant reduce of GB energy by 0.3 Jm^{-2} and increase of sliding barrier up to 0.3 Jm^{-2} . The disagreement between coupling factors of GB $\Sigma 5(210)$ obtained from sliding energy profiles in Fig. 1 and Fig. 2 is most probably caused by backward migration. Backward migration occurs, when GB plane returns to its previous position instead of migration to new position. Backward migration could be reduced by increase of supercell dimension in direction perpendicular to GB plane (sz). Test will be subject of our further research.

4. Conclusion

We have investigated the effect of vacancy on mechanical properties of bcc-iron $\langle 100 \rangle$ symmetric tilt GBs $\Sigma 5(210)$, $\Sigma 5(310)$, $\Sigma 17(410)$ and $\Sigma 13(510)$. Namely, effect on grain boundary energy, sliding barrier and coupling factor. Clear effect of vacancy was identified only on coupling factor. Based on our semi-empirical simulations, the increase of coupling factor due to the presence of vacancy on GB plane was observed. As a consequence, vacancy segregation on GB plane reduce GB motion in the direction perpendicular to GB plane. Effect of vacancy on sliding barrier differs according to GB type and therefore requires further research.

Acknowledgement

This work was supported by Structural Funds of the European Union by means of the Research Agency of the Ministry of Education, Science, Research and Sport of the Slovak Republic in the project "CENTE I" ITMS code 26240120011 and by Scientific Grant Agency of the Ministry of Education of Slovak Republic and Slovak Academy of Sciences No. VEGA 1/0377/13.

References:

- [1] H. Zong, et al.: *Acta Materialia*, **82**, 295 (2015).
- [2] B. Hyde, D. Farkas and M. J. Caturla: *Philosophical Magazine*, **85**, 3795 (2005).
- [3] H-B. Zhou, et al.: *Journal of Applied Physics*, **109**, 113512 (2011).
- [4] M. Wu, J. Gu and Z. Jin: *Scripta Materialia*, **107**, 75 (2015).
- [5] P. Ballo, J. Degmová and V. Slugeň: *Physical Review B*, **72**, 064118 (2005).
- [6] M. S. Daw and M. I. Baskes: *Physical Review B*, **29**, 6443 (1984).
- [7] M. I. Mendeleev, et al.: *Philosophical Magazine*, **83**, 3977 (2003).
- [8] D. Terentyev and X. He.: SCK•CEN, Mol, Belgium, BLG-1072 (2010).
- [9] M. Tschopp et al.: *Physical Review B*, **85**, 064108 (2012).